AIP Applied Physics Letters

Joule heating-induced coexisted spin Seebeck effect and spin Hall magnetoresistance in the platinum/Y3Fe5O12 structure

W. X. Wang, S. H. Wang, L. K. Zou, J. W. Cai, Z. G. Sun, and J. R. Sun

Citation: Applied Physics Letters **105**, 182403 (2014); doi: 10.1063/1.4901101
View online: http://dx.doi.org/10.1063/1.4901101
View Table of Contents: http://scitation.aip.org/content/aip/journal/apl/105/18?ver=pdfcov
Published by the AIP Publishing

APPLIED PHYSICS LETTERS **105**, 182403 (2014)

Joule heating-induced coexisted spin Seebeck effect and spin Hall magnetoresistance in the platinum/$Y_3Fe_5O_{12}$ structure

W. X. Wang,[1,2] S. H. Wang,[2] L. K. Zou,[2] J. W. Cai,[2] Z. G. Sun,[1] and J. R. Sun[2,a)]
[1]*State Key Laboratory of Advance Technology for Material Synthesis and Processing, Wuhan University of Technology, Wuhan 430070, China*
[2]*Beijing National Laboratory for Condensed Matter Physics and Institute of Physics, Chinese Academy of Sciences, Beijing 100190, People's Republic of China*

(Received 10 September 2014; accepted 24 October 2014; published online 4 November 2014)

Spin Seebeck effect (SSE) and spin Hall magnetoresistance (SMR) are observed simultaneously in the Pt/$Y_3Fe_5O_{12}$ hybrid structure when thermal gradient is produced by Joule heating. According to their dependences on applied current, these two effects can be separated. Their dependence on heating power and magnetic field is systematically studied. With the increase of heating power, the SSE enhances linearly, whereas the SMR decreases slowly. The origin of the spin currents is further analyzed. The heating power dependences of the spin currents associated with the SSE and the SMR are found to be different. © *2014 AIP Publishing LLC*.
[http://dx.doi.org/10.1063/1.4901101]

The exploration for effective approaches for the generation, detection, and manipulation of spin current has been a focus of spintronics.[1] It was recently reported that the spin Seebeck effect (SSE) can provide a feasible approach to generate stabilized spin current:[2,3] When a temperature gradient ∇T is established along the ferromagnet (FM), a spin current will be formed along the FM. This spin current can be detected by a noble metal (NM) and converted into a voltage via inverse spin Hall effect (ISHE).[4] Since platinum has a strong spin-orbit coupling, thus a strong ISHE, it is usually utilized as a detector of the spin current. The SSE has been observed in a wide variety of materials, including magnetic conductors,[3] semiconductors,[5] and magnetic insulators.[6,7] Based on the SSE, a concept of spin caloritronics has been presented, and it has received a worldwide attention in recent years.[8]

Longitudinal geometry is the simplest experimental setup for the SSE study,[6] for which the thermal gradient was established by either attaching a heat source and a heat sink, respectively, to the two ends of the sample,[3,5,6] locally heating the sample by a laser beam,[9] or applying a current through the NM.[10] In the first case, a good thermal contact between the heat reservoirs and the samples is required. While in the case of laser heating, the temperature gradient exists only in a very local region. Based on Joule heating, Schreier *et al.*[10] suggested a new method to generate thermal gradient. Because of its feasibility and controllability, this method shows obvious advantages over the other two ones.

As reported, magnetic proximity effect[11] and charge and spin current interaction exist in the Pt/$Y_3Fe_5O_{12}$ (YIG) hybrid structure. Therefore, one must be careful when dealing with the SSE in this kind of structure. According to Miao *et al.*,[12] the magnetoresistance (MR) of Pt/YIG could be mainly ascribed to the spin current reflection at the Pt/YIG interface in low magnetic fields and to the proximity effect under high fields. The former is called spin Hall magnetoresistance (SMR), a new MR mechanism proposed by Nakayama *et al.*[11] According to Nakayama *et al.*,[11] the SMR is induced by a nonequilibrium proximity effect.[13,14] Due to the coexisted spin Hall effect and ISHE, the momentum exchange of the spin current at the Pt/YIG interface affects in return the resistance of the Pt strip. As a consequence, MR appears in Pt as the direction of the magnetization of YIG rotates. According to the above discussions, the SSE and SMR may appear simultaneously when establishing the thermal gradient by Joule heating. However, how to separate these two effects and their mutual influence remain unaddressed up to now despite the intensive studies on the respective SSE and SMR. In this letter, the accompanied SSE and SMR were reported for the Joule-heated Pt/YIG hybrid structure, and their respective dependences on heating power and magnetic fields are established. Differences of the spin accumulations associated with these two effects are discussed.

(111)-oriented $Gd_3Ga_5O_{12}$ (GGG) ($5 \times 3 \times 0.5\,mm^3$) was adopted as substrates and a 21-μm thick single crystal YIG slab was grown above the GGG by liquid phase epitaxy. Hall-bar-shaped Pt thin layers were deposited above the substrate by magnetron sputtering. Two typical layer thicknesses, $t_{Pt} = 7\,nm$ and 30 nm, were adopted for the present studies. The resistivity, ρ_{xx}, of the Pt films was $\sim 2.4 \times 10^{-7}$ Ω m for $t_{Pt} = 7\,nm$ and $\sim 1.5 \times 10^{-7}$ Ω m for $t_{Pt} = 30\,nm$ at the room temperature, measured by the standard four-probe technique. A Pt(7 nm)/Cu(3 nm)/YIG sample was also prepared for comparison study, where the Cu buffer layer was introduced to depress the magnetic proximate effect. The samples were mounted on a heat sink (copper) with thermally conductive adhesive, and sealed in an electromagnetic shielding box. The electric measurements were performed under the ambient conditions.

Figure 1(a) shows a schematic illustration of the experimental setup. A large current I was applied along the long dimension of the Pt film to establish a thermal gradient along the z direction of the sample, and a magnetic field was applied in the sample plane at an angle of θ with respect to I

a)Author to whom correspondence should be addressed. Electronic addresses: jrsun@iphy.ac.cn and sun_zg@whut.edu.cn

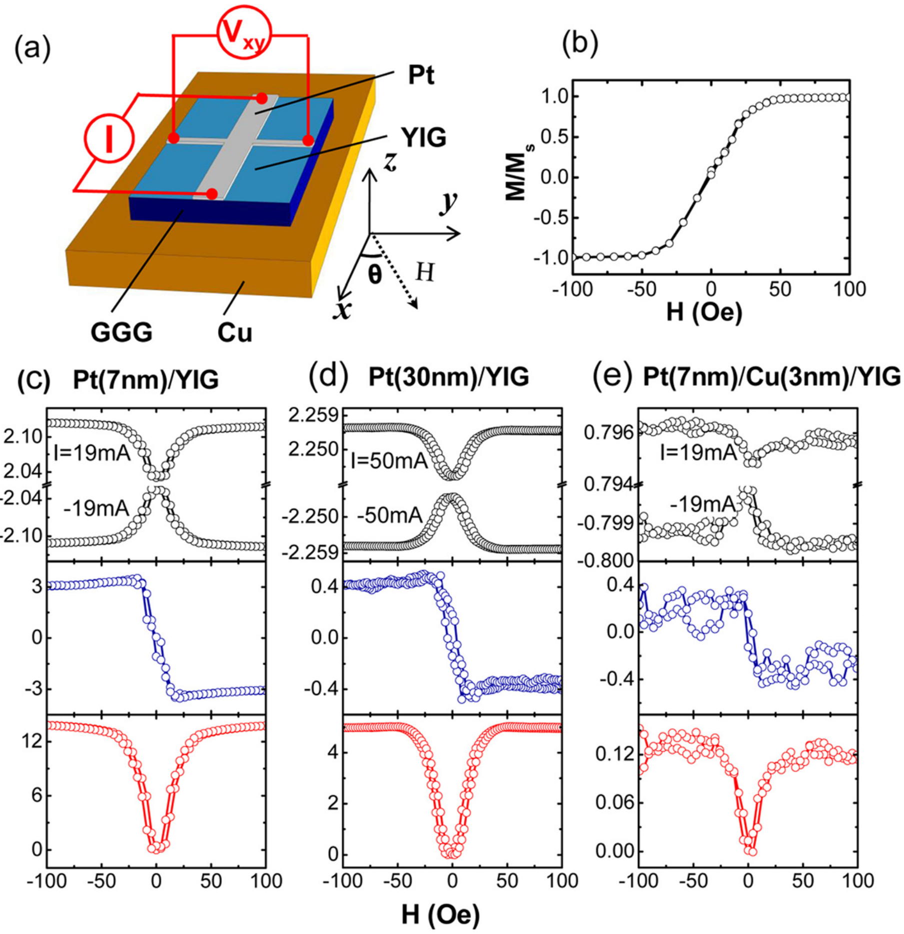

FIG. 1. (a) A schematic illustration of the experimental setup. A current I is applied to the Pt strip and the Joule heat induced temperature gradient ∇T is established in the z direction of the YIG. (b) Normalized magnetization of YIG, presented as a function of magnetic field. (c), (d), and (e) Magnetic field dependences of the transverse voltage V_{xy} (black curve), V_{ISHE} (blue curve), and MR (red curve) for the samples of Pt(7 nm)/YIG, Pt(30 nm)/YIG, and Pt(7 nm)/Cu(3 nm)/YIG, respectively. The measurements were performed with the applied currents of ± 19 mA for Pt(7 nm)/YIG and Pt(7 nm)/Cu(3 nm)/YIG, and ± 50 mA for Pt(30 nm)/YIG. Here, the magnetic field is applied in the sample plane at an angle of $\theta = 45°$ with respect to the current direction.

to orient the magnetic moment of the YIG. A transverse voltage V_{xy} was then produced and recorded. In general, the thermal gradient induced by Joule heating will generate a spin current injection into Pt, thus the SSE. In addition to the SSE, according to Nakayama *et al.*, the spin current reflection at the Pt/YIG interface may also produce a SMR in Pt, yielding a voltage change along the y-direction of the Pt stip. In addition to SMR, the conventional anisotropic magnetoresistance (AMR) is also possible when the proximate effect is strong. Obviously, the SSE will remain unaffected whereas the MR effect, either the SMR or the AMR, changes sign while current direction reverses. Since V_{ISHE} is simply proportional to heating power ($P = I^2 R_{xx}$), we have the following relations $V_{\mathrm{ISHE}}(I) = V_{\mathrm{ISHE}}(-I)$ and $V_{\mathrm{MR}}(I) = -V_{\mathrm{MR}}(-I)$, or $V_{\mathrm{ISHE}} = [V_{xy}(I) + V_{xy}(-I)]/2$ and $V_{\mathrm{MR}} = [V_{xy}(I) - V_{xy}(-I)]/2$, i.e., from their different dependences on oppositely directed currents, the V_{ISHE} and the MR can be distinguished from each other.

The SSE and MR effect of the Pt/YIG structure were studied by cycling magnetic field along the route $-0.01\,\mathrm{T} \rightarrow 0.01\,\mathrm{T} \rightarrow -0.01\,\mathrm{T}$. The measurement begins about 20 min after the application of the heating current, when a steady thermal gradient is established. Figs. 1(c) and 1(d) show the magnetic field dependence of V_{xy} (black lines), V_{ISHE} (blue lines), and MR (red lines), obtained by applying magnetic field at an angle of $\theta = 45°$, here, the MR is defined as $[V_{\mathrm{MR}}(H)–V_{\mathrm{MR}}(0)]t_{\mathrm{Pt}}/I\rho_{xx}(H)$. To compare the effect of current reversion, both data obtained under I and $-I$ are presented. Notably, the V_{xy} exhibits a strong field dependence in the low field region, which is the signature of the MR, as first reported by Ref. 11. A V_{xy} peak appears around $H = 0$, with a small hysteresis for the ascending-descending field operations. According to Fig. 1(b), this is exactly the field range for the magnetic reorientation of YIG. The V_{xy}–H curves are upside down when the current direction is reversed, indicating that the MR governs the V_{xy}. Above the saturation field, V_{xy} is nearly constant. This is understandable since the YIG has been magnetically saturated. There is a misalignment for the base lines of the V_{xy}–H curves under the positive and negative fields. This is a signature of the SSE, which contributes a V_{ISHE} which changes sign as the magnetic alignment of the YIG reverses.

To get a quantitative characterization of the SSE, in Figs. 1(c) and 1(d), we show the V_{ISHE}–H relations (blue curves). As expected, V_{ISHE} is nearly constant when H is high, and undergoes a sudden drop/jump as H sweeps through the saturation field of YIG; the magnetic reversion of YIG causes the V_{ISHE} change. A simple analysis indicates that the V_{ISHE} is $\sim 3\,\mu$V for Pt(7 nm)/YIG and $\sim 0.42\,\mu$V for Pt(30 nm)/YIG. There are two possible explanations for the reduced V_{ISHE} in the latter sample, i.e., the thick Pt has shunted the V_{ISHE} or the thermal gradient in these two samples are different. It is possible that the thermal gradient produced by Joule heating in YIG is inhomogeneous, concentrating near the Pt/YIG interface. The small V_{ISHE}–H loop can be ascribed to the magnetic hysteresis of the YIG.

The MR is also shown in Figs. 1(c) and 1(d) (red curves). It grows rapidly with H when the field is low, and saturates, above the field of ~50 Oe, at the value of ~0.014% for $t_{Pt} = 7$ nm and ~0.0048% for $t_{Pt} = 30$ nm. The decrease of the MR with the increase of t_{Pt} is consistent with the previously reported results.[11]

As mentioned above, either the SMR or the AMR may contribute to MR. According to Nakayama *et al.*, the SMR could be the main mechanism determining the MR for the Pt/YIG hybrid structure. According to Miao *et al.*,[12] the magnetic proximity effect, thus the AMR prevails under high fields. To reveal the origin of the MR observed here, the MR of the Pt(7 nm)/Cu(3 nm)/YIG structure is studied under the same condition as that of Pt(7 nm)/YIG. Fig. 1(e) shows that the MR remains without the proximate effect, though its magnitude reduces due to the short-circuit effect of the highly conductive Cu layer. Since Cu has a long spin diffusion length and a very weak spin-orbit coupling, it can carry a spin current over a long distance but prevents the magnetization of the Pt layer by proximate effect. Based on a simple calculation, we show that the short-circuit effect of a 3-nm-thick Cu layer reduces the MR by a factor of ~50, while the experimentally observed reduction is by a factor of ~90. Considering the possible influence of the Cu layer on spin current, this agreement is satisfactory. Combining the results in Fig. 1 with those in Refs. 11 and 12, we concluded that the MR observed in our samples is dominated by SMR, i.e., the SSE and SMR coexist in the Joule-heated Pt/YIG hybrid structure.

To compare with the effect of Joule heating, we also measure the SSE for a vertical structure when the thermal gradient is established by a heater underneath the GGG. Fig. 2(a) shows the experimental setup, and Fig. 2(b) is the experimental results. Two features can be identified from the data in Fig. 2(b). First, the sign of the V_{ISHE} produced by underneath heating is opposite to that of the V_{ISHE} caused by Joule heating, indicating that the temperature gradient in these two cases is opposite. Second, the V_{ISHE} value, which is ~0.15 μV for Pt(7 nm)/YIG and ~0.10 μV for Pt(30 nm)/YIG, is much lower than that produced by Joule heating. It means that the Joule heating is more effective in producing thermal gradient. One thing deserving special attention is that the difference of the V_{ISHE} for the Pt(7 nm)/YIG and Pt(30 nm)/YIG is smaller than that observed in the case of Joule heating (Figs. 1(c) and 1(d)). Provided that the thermal gradient in the case of underneath heating is similar for two samples, the thermal gradient caused by Joule heating could be different, though the heating power is similar.

To reveal the physical origin of the thermoelectric signals, we studied the V_{xy}–H relations when magnetic field is applied at different angles. In Figs. 3(a) and 3(b), we show the V_{ISHE} and ρ_{xy} values deduced from the V_{xy}–H relations for $\theta = 0°$, 45°, 90°, 135°, and 180°, respectively. Obviously, the V_{ISHE} exhibits a strong dependence on θ. It is maximal for $\theta = 0°$ and 180° and minimal for $\theta = 90°$, varying in the form of $k_0\cos\theta$, where $k_0 = 4\,\mu$V for Pt(7 nm)/YIG, 0.76 μV for Pt(30 nm)/YIG, and 0.39 μV for Pt(7 nm)/Cu(3 nm)/YIG (Fig. 3(c)). In contrast, the SMR takes the maximal values at $\theta = 45°$ and 135° and the minimal values at $\theta = 90°$, 0°, and 180°. A further analysis indicates that SMR exhibits a $k_1\sin 2\theta$ variation with θ (Fig. 3(d)), similar to that observed by Nakayama *et al.*[11] The fitting parameters are $k_1 = 2 \times 10^{-4}$ for Pt(7 nm)/YIG, 5×10^{-5} for Pt(30 nm)/YIG, and 1.2×10^{-6} for Pt(7 nm)/Cu(3 nm)/YIG. Obviously, the V_{ISHE}–H and ρ_{xy}–H relations own the typical features of the SSE and SMR, respectively.

The above experiment results indicate that when the thermal gradient is established by Joule heating, the SSE and SMR coexist, and can be separated and analyzed

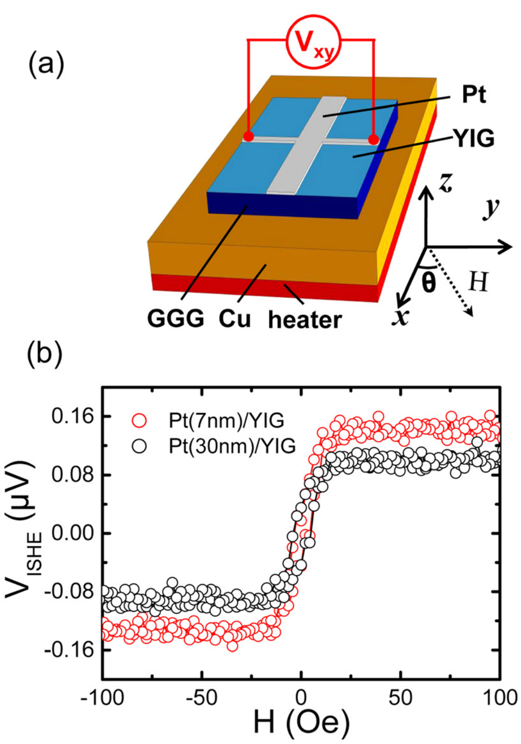

FIG. 2. (a) A schematic illustration of the experimental setup. (b) V_{ISHE} signals as functions of magnetic field.

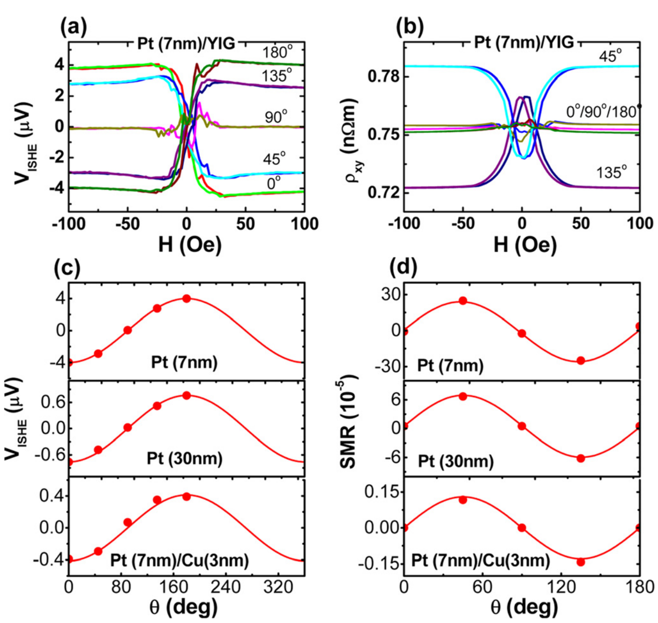

FIG. 3. (a) and (b) Magnetic field dependence of the V_{ISHE} and ρ_{xy} for the sample of Pt(7 nm)/YIG, measured at different angles. Labels in the figure mark the values of θ. (c) and (d) angular dependence of V_{ISHE} and SMR for Pt(7 nm)/YIG, Pt(30 nm)/YIG, and Pt(7 nm)/Cu(3 nm)/YIG. Solid lines are results of theoretical calculation based on the cos θ or sin2θ dependence, and symbols are experiment data.

independently. To get an idea about the effect of heating power $P = I^2R$, in Figs. 4(a) and 4(b), we show V_{ISHE} and SMR as functions of P. As expected, the V_{ISHE} exhibits a linear growth with P: Heating power enhances the spin current by increasing thermal gradient. Fascinatingly, V_{ISHE} displays a much more rapid increase with the increase of P for the sample of $t_{\mathrm{Pt}} = 7\,\mathrm{nm}$ than for $t_{\mathrm{Pt}} = 30\,\mathrm{nm}$, indicating that the thinner sample is more sensitive to Joule heating. Different from V_{ISHE}, SMR undergoes a slight decrease with P. This temperature dependence of the SMR can be theoretically explained.[13,15] According to Chen *et al.*,[13] the maximum SMR can be described by

$$SMR = \theta_{sh}^2 \frac{\lambda}{t_{Pt}} \frac{2\lambda G \tanh^2\left(\frac{t_{Pt}}{2\lambda}\right)}{\sigma + 2\lambda G t \coth\left(\frac{t_{Pt}}{\lambda}\right)}, \qquad (1)$$

where λ is the spin diffusion length, θ_{sh} is the spin Hall angle, G is the spin mixing conductance, and σ is the conductivity of Pt. Noting that λ is a function of temperature, $\lambda \propto 1/T$ according to the Elliot-Yafet assumption, one finds that the SMR will decrease with the increase of temperature.[15] Therefore, the slight decrease of the MR with temperature is the further evidence of the SMR effect. It suggests that this effect is closely related to the bulk spin-orbital coupling in Pt, stemming from the reduction of the spin diffusion length at high temperatures. This observation is particularly interesting since it is helpful in distinguishing the SMR from the effect caused by the Rashba spin-orbital coupling at the Pt/YIG interface, as shown recently by Grigoryan *et al.*[16]

Finally, we would like to present a brief discussion about the spin currents that are responsible for the SSE and the SMR. Although the ISHE plays an important role in causing both the SSE and the SMR, the mechanisms for the

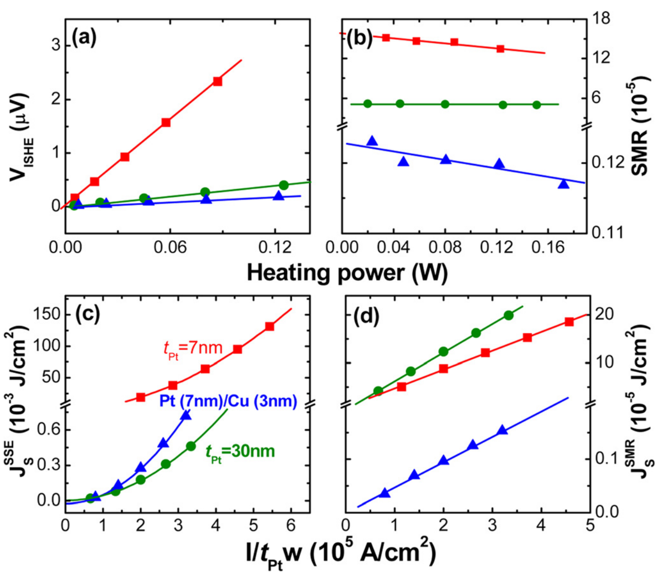

FIG. 4. (a) and (b) Effect of heating power (P) on the V_{ISHE} (a) and the SMR (b). (c) Relations between spin current J_S^{SSE} and applied current I. (d) Relations between spin current J_S^{SMR} and applied current I. Solid lines in (a), (b), and (d) are guides for the eye. Solid lines in (c) are the results fitting to the equation of $J_S^{SSE} = \alpha I^2$.

spin accumulation in these two cases are different. As formulated, the spin current density that causes the SSE has the form[17,18]

$$J_S^{SSE} = \frac{\Delta V_{\mathrm{ISHE}}}{C\eta}\frac{1}{w}, \qquad (2)$$

where C is the open-circuit spin Hall conversion efficiency,[17,18] η is a correction factor,[17,19] and w is the width of the Pt strip. C and η can be further expressed as

$$C = \frac{2e}{\hbar}\theta_{sh}\lambda \tanh\left(\frac{t_{Pt}}{2\lambda}\right)\frac{\sigma}{t_{Pt}}, \qquad (3)$$

$$\eta = \left[1 + 2G\sigma\lambda\frac{e^2}{h}\coth\left(\frac{t_{Pt}}{2\lambda}\right)\right]^{-1}. \qquad (4)$$

In contrast, the spin current associated with the SMR has the form[14,17]

$$J_S^{SMR} = SMR\frac{I\hbar}{\theta_{sh} e\lambda w \tanh\left(\frac{t_{Pt}}{2\lambda}\right)}. \qquad (5)$$

Adopting the representative parameters of the Pt/YIG hybrid structure, $G = 1 \times 10^{19}\,\mathrm{m}^{-2}$, $\theta_{sh} = 0.11$, and $\lambda = 1.5\,\mathrm{nm}$, the J_S^{SSE} and J_S^{SMR} can be directly calculated. We show the J_S^{SSE}–I relation in Fig. 4(c) and the J_S^{SMR}–I relation in Fig. 4(d). Both J_S^{SSE} and J_S^{SMR} have the values similar to those as previously reported.[16] The J_S^{SSE} exhibits a quadratic dependence on I, which is understandable since ∇T is proportional to I^2R. However, the J_S^{SMR} essentially linearly grows with I, indicating that the effect of temperature is not strong. This result is consistent with the data in Fig. 4(b). According to the above analyses, obviously, the spin accumulation stems from thermal gradient for the SSE, whereas it is caused by the spin transfer torque of dc current at the Pt/YIG interface for the SMR.

In summary, we demonstrate that the current heating is a convenient and effective method to produce the SSE. Due to the nonequilibrium proximity effect of the Pt film, moreover, the heating current induces simultaneously a SMR, an effect jointly produced by the Spin Hall effect and the inverse spin Hall effect. With the increase of heating power, the SSE enhances linearly whereas the SMR decreases slowly. The origin of the spin currents is further analyzed, and different dependences on heating current are observed for the spin currents associated with the SSE and SMR, indicating that the spin accumulation are different for these two effects.

This work has been supported by the National Basic Research of China (Grant Nos. 2011CB921801 and 2012CB921403) and the National Natural Science Foundation of China (Grant Nos. 11174231, 11074285, 51372064, and 11134007).

[1]H. Ohno, Nat. Mater. **9**, 952 (2010).
[2]J. C. Le Breton, S. Sharma, H. Saito, S. Yuasa, and R. Jansen, Nature **475**, 82 (2011).

[3]K. Uchida, S. Takahashi, K. Harii, J. Ieda, W. Koshibae, K. Ando, S. Maekawa, and E. Saitoh, Nature **455**, 778 (2008).
[4]A. Azevedo, L. H. Vilela Leão, R. L. Rodriguez-Suarez, A. B. Oliveira, and S. M. Rezende, J. Appl. Phys. **97**, 10C715 (2005).
[5]C. M. Jaworski, J. Yang, S. Mack, D. D. Awschalom, J. P. Heremans, and R. C. Myers, Nat. Mater. **9**, 898 (2010).
[6]K. Uchida, J. Xiao, H. Adachi, J. Ohe, S. Takahashi, J. Ieda, T. Ota, Y. Kajiwara, H. Umezawa, H. Kawai, G. E. W. Bauer, S. Maekawa, and E. Saitoh, Nat. Mater. **9**, 894 (2010).
[7]K.-i. Uchida, H. Adachi, T. Ota, H. Nakayama, S. Maekawa, and E. Saitoh, Appl. Phys. Lett. **97**, 172505 (2010).
[8]G. E. W. Bauer, E. Saitoh, and B. J. van Wees, Nat. Mater. **11**, 391 (2012); F. L. Bakker, A. Slachter, J. P. Adam, and B. J. van Wees, Phys. Rev. Lett. **105**, 136601(2010); M. Hatami, G. E. W. Bauer, Q. F. Zhang, and P. Kelly, Phys. Rev. Lett. **99**, 066603 (2007); M. Johnson and R. Silsbee, Phys. Rev. B **35**, 4959 (1987); A. Slachter, F. L. Bakker, J. P. Adam, and B. J. van Wees, Nat. Phys. **6**, 879 (2010).
[9]M. Weiler, M. Althammer, F. D. Czeschka, H. Huebl, M. S. Wagner, M. Opel, I.-M. Imort, G. Reiss, A. Thomas, R. Gross, and S. T. B. Goennenwein, Phys. Rev. Lett. **108**, 106602 (2012).
[10]M. Schreier, N. Roschewsky, E. Dobler, S. Meyer, H. Huebl, R. Gross, and S. T. B. Goennenwein, Appl. Phys. Lett. **103**, 242404 (2013).
[11]H. Nakayama, M. Althammer, Y. T. Chen, K. Uchida, Y. Kajiwara, D. Kikuchi, T. Ohtani, S. Geprägs, M. Opel, S. Takahashi, R. Gross, G. E. W. Bauer, S. T. B. Goennenwein, and E. Saitoh, Phys. Rev. Lett. **110**, 206601 (2013).
[12]B. F. Miao, S. Y. Huang, D. Qu, and C. L. Chien, Phys. Rev. Lett. **112**, 236601 (2014).
[13]Y. T. Chen, S. Takahashi, H. Nakayama, M. Althammer, S. Goennenwein, E. Saitoh, and G. E. W. Bauer, Phys. Rev. B **87**, 144411 (2013).
[14]M. Althammer, S. Meyer, H. Nakayama, M. Schreier, S. Altmannshofer, M. Weiler, H. Huebl, S. Geprägs, M. Opel, R. Gross, D. Meier, C. Klewe, T. Kuschel, J. M. Schmalhorst, G. Reiss, L. Shen, A. Gupta, Y. T. Chen, G. E. W. Bauer, E. Saitoh, and S. T. B. Goennenwein, Phys. Rev. B **87**, 224401 (2013).
[15]S. R. Marmion, M. Ali, M. McLaren, D. A. Williams, and B. J. Hickey, Phys. Rev. B **89**, 220404 (2014).
[16]V. L. Grigoryan, W. Guo, G. E. W. Bauer, and J. Xiao, Phys. Rev. B **90**, 161412(R) (2014).
[17]M. Weiler, M. Althammer, M. Schreier, J. Lotze, M. Pernpeintner, S. Meyer, H. Huebl, R. Gross, A. Kamra, J. Xiao, Y. T. Chen, H. J. Jiao, G. E. W. Bauer, and S. T. B. Goennenwein, Phys. Rev. Lett. **111**, 176601 (2013).
[18]F. D. Czeschka, L. Dreher, M. S. Brandt, M. Weiler, M. Althammer, I. M. Imort, G. Reiss, A. Thomas, W. Schoch, W. Limmer, H. Huebl, R. Gross, and S. T. B. Goennenwein, Phys. Rev. Lett. **107**, 046601 (2011).
[19]H. J. Jiao and G. E. W. Bauer, Phys. Rev. Lett. **110**, 217602 (2013).